Structural Engineering and Mechanics, *Vol. 51, No. 2 (2014) 315-331*
DOI: http://dx.doi.org/10.12989/sem.2014.51.2.315

Vibration of vehicle-bridge coupling system with measured correlated road surface roughness

Wanshui Han*[1], Sujing Yuan[2] and Lin Ma[3]

[1]*Department of Bridge Engineering, Chang'an University, Xi'an 710064, China*
[2]*School of Civil Engineering, Southeast University, Nanjing 210096, China*
[3]*Department of Civil Engineering, Hohai University, Nan'jing 210098, China*

(Received December 26, 2011, Revised May 13, 2014, Accepted May 18, 2014)

Abstract. The present study investigated the effect of the correlation of the measured road roughness profiles corresponding to the left and right wheels of a vehicle on the vibration of a vehicle-bridge coupling system. Four sets of road roughness profiles were measured by a laser road-testing vehicle. A correlation analysis was carried out on the four roughness samples, and two samples with the strongest correlation and weakest correlation were selected for the power spectral density, autocorrelation and cross-correlation analyses. The scenario of a three-axle truck moving across a rigid-frame arch bridge was used as an example. The two selected road roughness profiles were used as inputs to the vehicle-bridge coupling system. Three different input modes were adopted in the numerical analysis: (1) using the measured road roughness profile of the left wheel for the input of both wheels in the numerical simulation; (2) using the measured road roughness profile of the right wheel for both wheels; and (3) using the measured road roughness profiles corresponding to left and right wheels for the input corresponding to the vehicle's left and right wheels, respectively. The influence of the three input modes on the vibration of the vehicle-bridge system was analyzed and compared in detail. The results show that the correlation of the road roughness profiles corresponding to left and right wheels and the selected roughness input mode both have a significant influence on the vibration of the vehicle-bridge coupling system.

Keywords: vehicle-bridge coupling system; measured road surface roughness; correlation analysis; autocorrelation; roughness input modes

1. Introduction

In the past two decades, the effect of road surface roughness on the vibration of vehicle-bridge system has received considerable attention (Guo and Xu 2001, Wang and Huang 1992, Yang *et al.* 2009). The road surface roughness is one of the three most important factors in a vehicle-bridge coupling system with the other two factors being the dynamic properties of the vehicle and dynamic properties of the bridge. It is regarded as the main stimulus for the vibration of the coupling system, making it the key factor for the safety and comfort of the vehicle, dynamic response of the bridge, and the damages and failures of the structural components of the bridge (Xu and Guo 2004, Wang *et al.* 2005, Obrien *et al.* 2006, Ding *et al.* 2009, Zhu *et al.* 2014).

*Corresponding author, Associate Professor, E-mail: hws@gl.chd.edu.cn

http://www.techno-press.org/?journal=sem&subpage=8 ISSN: 1225-4568 (Print), 1598-6217 (Online)

There are two approaches of investigating the road surface roughness problem when analyzing the vehicle-bridge vibration problem, namely, the numerical simulation approach (Wang and Huang 1992) and the field test approach (Calcada *et al.* 2005, Cai *et al.* 2007). Most studies have been conducted using the numerical simulation methods, in which the road surface profile is usually assumed to be a zero-mean stationary Gaussian random process and can be generated through an inverse Fourier transformation based on a power spectral density (PSD) function (Dodds and Robson 1973). In addition, the difference of the road surface roughness in the transverse direction, i.e., the difference between the road roughness profiles corresponding to the left and right wheel tracks of a vehicle, was usually ignored (Au *et al.* 2001, Kim *et al.* 2007).

The random feature of the road surface roughness in the transverse direction has also been investigated by some researchers. Huang *et al.* (1992) generated two completely independent longitudinal road roughness profiles along each wheel track and used the two roughness profiles as separate input to left and right wheels of a vehicle. Based on an auto-regressive and moving average (ARMA) approach, Liu *et al.* (2002) created two random road surface profiles corresponding to the left and right wheels of a vehicle and investigated the influence of the correlation coefficient of the two random road surface profiles on the dynamic impact factor. In their study, an exponential correlation model was employed to reflect the spatial correlation of the multi-correlated road surface roughness profiles and a set of coefficients of correlation ranging from -0.9 to 0.9 were used in the parametric study. However, the exponential correlation model in transverse direction and the assumed range of (-0.9 0.9) for the coefficient of correlation were not validated in their study. Moreover, the difference between the power spectral density (PSD) functions of left and right wheels were not considered either.

Field tests have also been conducted to measure the real road surface roughness (Calcada *et al.* 2005, Cai *et al.* 2007). The road surface roughness profiles corresponding to the left and right wheel tracks were measured and used as the inconsistent input to the left and right wheels when studying the vehicle-bridge vibration problem. However, previous studies based on field tests were limited to calibrating and validating the proposed numerical vehicle-bridge coupling systems. The properties of road roughness profiles corresponding to the left and right wheels, such as power spectral density (PSD) function, correlation, autocorrelation and cross-correlation were not investigated. Furthermore, most previous studies used the same road surface roughness profile as input to vehicle's left and right wheels, meaning that the random feature of the road surface roughness in the transverse direction was ignored.

This paper analyzed the correlation between measured road roughness profiles corresponding to the left and right wheel track and investigated the effect of road roughness input mode on the vibration of a vehicle-bridge coupling system. The road surface roughness was measured with a laser road-testing vehicle and four sets of longitudinal roughness profiles were obtained. Correlation analysis of the roughness profiles was carried out and two profiles with the strongest correlation and weakest correlation were selected for the power spectral density, autocorrelation and cross-correlation analyses. A multi-rib rigid-frame arch bridge with a span length of 40 m was selected as an example in the numerical simulation and the influence of roughness input mode on vehicle-bridge coupling system was investigated. Three different input modes were adopted in the numerical analysis: (1) using the measured road roughness profile of left wheel for input of both wheels in the numerical simulation; (2) using the measured road roughness profile of right wheel for both wheels; and (3) using the measured road roughness profiles corresponding to left and right wheels for input corresponding to the vehicle's left and right wheels, respectively. For the purpose of convenience, the first two modes will be referred to as "consistent input mode" and the third

Fig. 1 Laser road-testing vehicle

Table 1 Correlation coefficient of the measured road surface roughness

	Profile 1	Profile 2	Profile 3	Profile 4
Correlation coefficient	0.8778	0.7473	0.3754	0.0988

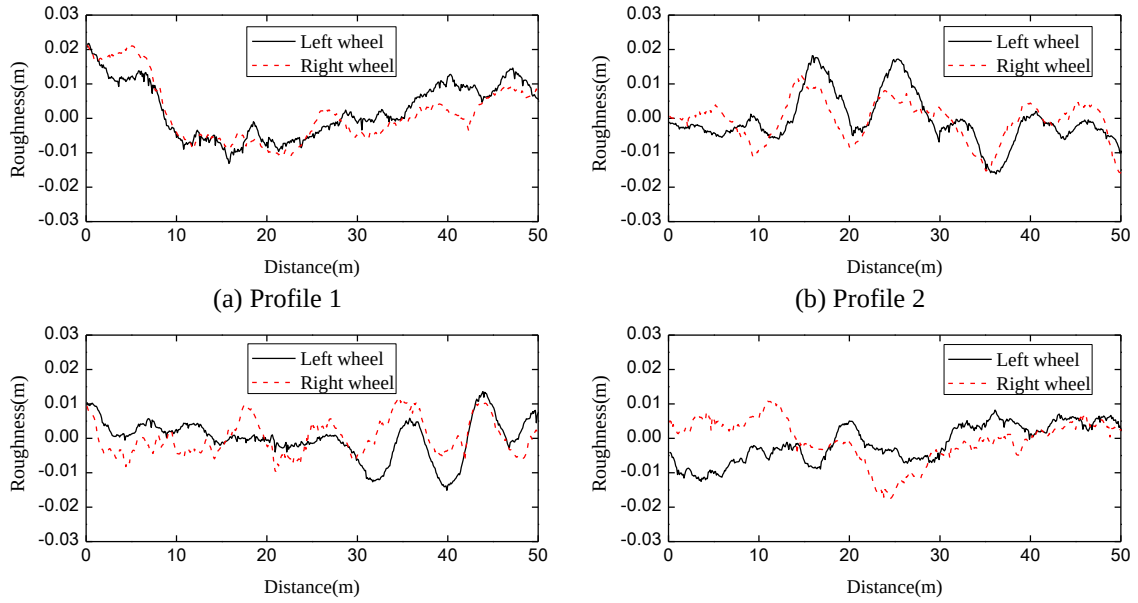

(a) Profile 1 (b) Profile 2

(c) Profile 3 (d) Profile 4

Fig. 2 Measured roughness profiles

mode will be referred to as "inconsistent input mode" hereafter.

2. Measurement and analysis of road surface roughness

The road surface roughness was measured by a laser road-testing vehicle (see Fig. 1), which measures the longitudinal roughness profiles along both the left and right wheel tracks of the vehicle. Fig. 2 shows four sets of the measured longitudinal roughness profile of a highway bridge,

where the data is sampled at an interval of 0.10 m.

In the theory of probability and statistics, correlation is a numerical measure of the strength of the linear relationship between two random variables. A correlation coefficient is a number between -1 and 1 that measures the degree to which two variables in consideration are linearly related. The larger the absolute value of the correlation coefficient is, the stronger their correlation is. For instance, a correlation coefficient of 1 denotes a very strong linear relationship between the two variables while a correlation coefficient of -1 denotes a strong but negative linear relationship. A correlation coefficient of 0 means that there is no linear relationship between the two variables. The correlation coefficients between the road roughness profiles corresponding to the left and right wheels were computed for the four sets of measured roughness profile and the results are presented in Table 1.

As shown in Table 1, Profile 1 has the strongest correlativity with a correlation coefficient of 0.8778 while Profile 4 has the weakest correlativity with a correlation coefficient of 0.0988. In order to study the influence of the correlation of the road surface roughness profiles for the two wheels on vibration of the vehicle-bridge coupling system, Profiles 1 and 4, which have the strongest and weakest correlation, respectively, were selected as the input to vehicle-bridge coupling system.

An analysis on the power spectrum density (PSD) for Profiles 1 and 4 was conducted and comparisons with the PSD curves of ISO 8608 (1995) are shown in Fig. 3. The figures show that the grade of the measured roughness profiles can be classified between “very good” and “good”.

A correlation function indicates the degree of the correlation between instantaneous values at different time for sample function of stochastic vibration. An autocorrelation function describes the dependent relationship between different instantaneous amplitudes for the same sample function of stochastic vibration.

The autocorrelation function for two sets of road roughness profiles selected is shown in Fig. 4. As indicated in the figure, the fluctuating trend in autocorrelation function curves of right and left wheels is consistent for Profile 1 while this is not the case for Profile 4.

Cross-correlation function describes the dependent relationship between different instantaneous amplitudes for two sample functions of stochastic vibration. The cross-correlation functions of the two selected road profiles are shown in Fig. 5. It can be observed from the figure that the cross

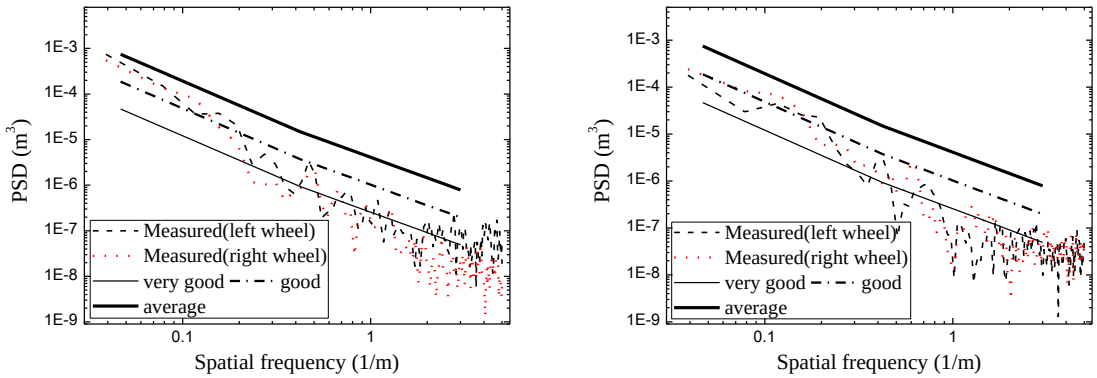

(a) Left and right wheels of Profile 1 (b) Left and right wheels of Profile 4

Fig. 3 PSD Analysis of measured roughness profiles and classification according to ISO 8608

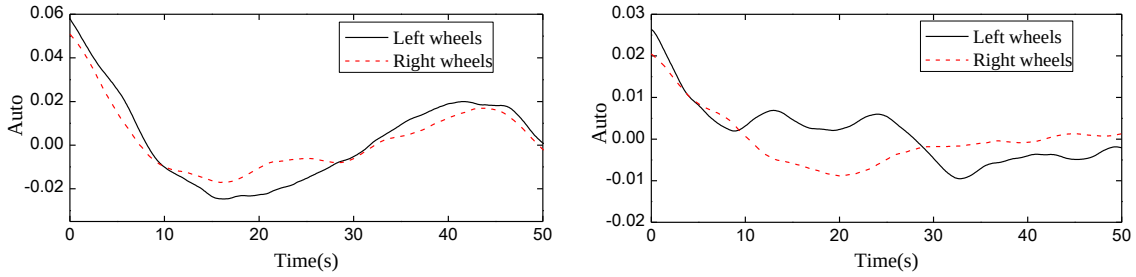

(a) Profile 1 (b) Profile 4

Fig. 4 Auto-correlation function

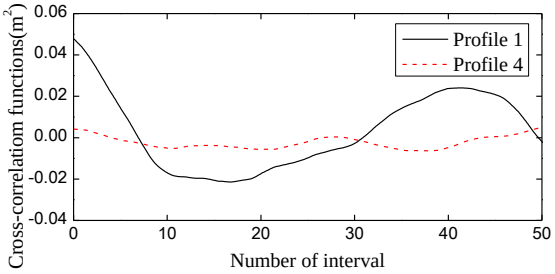

Fig. 5 Cross-correlation function

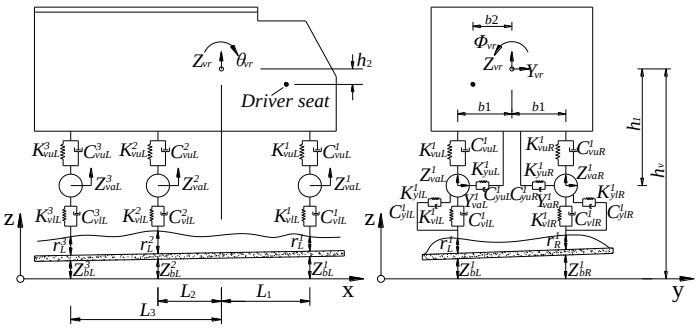

Fig. 6 Three-axle vehicle model

correlation of Profile 1 is relatively strong while cross-correlation function values of Profile 4 are close to '0'. Therefore, Profile 4 has weaker cross correlation between the two roughness profiles.

3. Vehicle-bridge coupling system for multi-girder bridge

3.1 Vehicle model

The vehicle model is simplified as a combination of rigid bodies connected by a series of springs and damping devices. During the static and dynamic load testing of bridge, the vehicle specified in *Load Test Methods of Long Span Concrete Bridge* (1982) was selected. This vehicle is a three-axle vehicle with gross weight of about 30t and the numerical model for this vehicle is

shown in Fig. 6. For the three-axle vehicle in Fig. 6, the entire vehicle consists of 7 rigid bodies and has 17 independent degrees of freedom (DOF), namely, six vertical and lateral DOFs for the six wheels, and one vertical, lateral, pitching, yawing and rolling DOF, respectively, for the vehicle body.

3.2 Coupling relationships between vehicle and bridge

In the bridge/vehicle interaction, the analytical model of bridge structures is established using the finite element method (FEM). There are mainly two kinds of element types used in the developed FEM software: one is three-dimensional spine beam for the simulation of bridge deck, pylon and pier, and the other one is truss element which is used for the simulation of cables and steel truss members. According to the determination method of displacement of the bridge at the tire-road contact points, the coupling relationships of bridge/vehicle interaction can be divided into the single-girder model and grillage model (Han 2006). The single girder bridge model is generally used for long span bridges with box cross sections and the grillage method is more suitable for the cross section which is composed of several I- or T-shaped sections. The grillage method can also be used in box girders, which can provide the transverse force distribution with a high accuracy.

The vertical force imposed by the left (right) wheel of the j th axle of the vehicle on the bridge deck can be expressed as

$$F_{vL(R)}^{j} = K_{vlL(R)}^{j}(Z_{vaL(R)}^{j} - Z_{bL(R)}^{j} - r_{L(R)}^{j}(x)) + C_{vlL(R)}^{j}(\dot{Z}_{vaL(R)}^{j} - \dot{Z}_{bL(R)}^{j} - \dot{r}_{L(R)}^{j}(x)) \tag{1}$$

where $K_{vlL(R)}^{j}$ and $C_{vlL(R)}^{j}$ are the lower spring stiffness coefficient and damping coefficient of the left (right) wheel of the j th axle of the vehicle, respectively; $Z_{vaL(R)}^{j}$ and $\dot{Z}_{vaL(R)}^{j}$ are the vertical displacements and velocities of left (right) wheel of the j th axle of the vehicle, respectively; $Z_{bL(R)}^{j}$ and $\dot{Z}_{bL(R)}^{j}$ are the vertical displacements and velocities of bridge at the contact points of the left (right) tire which are determined by interpolation of the nodes close to the contact point through finite element method; $\dot{r}_{L(R)}^{j}(x) = (dr_{L(R)}^{j}(x)/dx)\cdot(dx/dt) = dr_{L(R)}^{j}(x)/dx \cdot V(t)$ and $V(t)$ is the vehicle velocity.

3.3 Equations of motion and solutions

The interaction equation of the bridge and vehicles are shown as below.

$$\begin{bmatrix} M_v & 0 \\ 0 & M_b \end{bmatrix}\begin{Bmatrix} \ddot{u}_v \\ \ddot{u}_b \end{Bmatrix} + \begin{bmatrix} C_v & 0 \\ 0 & C_b \end{bmatrix}\begin{Bmatrix} \dot{u}_v \\ \dot{u}_b \end{Bmatrix} + \begin{bmatrix} K_v & 0 \\ 0 & K_b \end{bmatrix}\begin{Bmatrix} u_v \\ u_b \end{Bmatrix} = \begin{Bmatrix} F_{vg} + F_{vb} \\ F_{bv} \end{Bmatrix} \tag{2}$$

where, M, C and K are the mass, damping, and stiffness matrices, respectively; the subscripts v and b denote the vehicle and bridge, respectively; u represents the displacement vector; F_{vg} is the self-weight of the vehicle; F_{vb} is the vector of wheel-bridge contact forces acting on the vehicle; and F_{bv} is the wheel-bridge contact forces acting on the bridge.

According to the relative geometric relationships and interaction force relationships between the coupled vehicle and bridge subsystems, an iterative process was applied to ensure that the displacement and force compatibility conditions are satisfied at the vehicle-bridge contact points at each time step (Han 2006). In each iteration, the displacements of the contact points were assumed

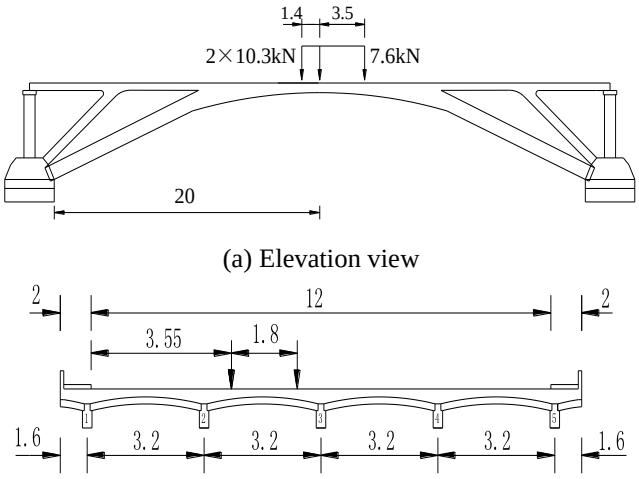

(a) Elevation view

(b) Cross section

Fig. 7 Configuration of the rigid-frame arch bridge

first, and the interaction forces between the vehicles and bridge were then calculated by solving the equations of motion of vehicles. If the interaction forces were in tension, it means the corresponding vehicle wheels have left the riding surface, and then the contact forces at the contact point were set to be zero. The updated displacements of the contact points were obtained by solving the equations of motion of bridge using the calculated interaction forces. The iteration process was finally terminated when the displacements of all the contact points from the two consecutive iterations were close enough with the threshold value set to 0.00001.

The vehicle-bridge coupling system analysis module was prepared adopting the above mentioned method based on Visual Fortran and embedded into the self-developed bridge dynamic analysis software BDANS (Bridge Dynamic Analysis System). In addition, BDANS has the program interface, pre and post processing system and animation demonstration systems, which can help to obtain the dynamic images of vehicle's driving across bridge and understand the computational process.

4. Case study

4.1 Bridge parameter

A rigid-frame arch bridge, with a span length of 40 m and a roadway width of 12 m, was used as an example in the numerical simulation in this study. The rise-to-span ratio of the bridge is l_0/f_0=1/10. The bridge has five arched rigid-frames, each consisting of an arch leg, diagonal brace, solid-web section, chord and transversal collar beam with a frame spacing of 3.2 m, which is shown in Fig. 7.

In the present study, the rigid-frame arch bridge was modeled with the BDANS using beam element. The first five natural frequencies and corresponding characteristics of mode shapes are summarized in Table 2.

Table 2 First five natural frequencies and mode shapes of the rigid-frame arch bridge

Order	Natural frequency [Hz]	Characteristics of mode shapes
1	4.2624	First order anti-symmetric vertical bending vibration
2	6.0213	First order symmetric vertical bending vibration
3	6.1461	First order symmetric torsional vibration
4	8.4296	In-deck transversal symmetric bending vibration of the bridge
5	9.3894	Out-of-deck symmetric bending vibration

Table 3 Major parameters of the vehicle under study

Parameter	Unit	Value
Full length of vehicle	m	7.78
Mass of truck body	kg	26807
Pitching moment of inertia of truck body	kg·m^2	10000
Rolling moment of inertia of truck body	kg·m^2	40000
Yawing moment of inertia of truck body	kg·m^2	100000
Mass of front axle set	kg	359.5
Mass of middle axle set	kg	595.5
Mass of back axle set	kg	542.5
Mass of tires	kg	0.0
Upper vertical spring stiffness (K^1_{vuL}= K^1_{vuR})	kN/m	1200
Upper lateral spring stiffness (K^1_{yuL}= K^1_{yuR})	kN/m	1000
Upper vertical spring stiffness (K^2_{vuL}= K^2_{vuR}= K^3_{vuL}= K^3_{vuR})	kN/m	2400
Upper lateral spring stiffness (K^2_{yuL}= K^2_{yuR}= K^3_{yuL}= K^3_{yuR})	kN/m	1600
Upper vertical damper damping coefficient (C^1_{vuL}= C^1_{vuR})	kN·s/m	5.0
Upper lateral damper damping coefficient (C^1_{yuL}= C^1_{yuR})	kN·s/m	5.0
Upper vertical damper damping coefficient (C^2_{vuL}= C^2_{vuR}= C^3_{vuL}= C^3_{vuR})	kN·s/m	10.0
Upper lateral damper damping coefficient(C^2_{yuL}= C^2_{yuR}= C^3_{yuL}= C^3_{yuR})	kN·s/m	10.0
Lower vertical spring stiffness (K^1_{vlL}= K^1_{vlR})	kN/m	2400
Lower lateral spring stiffness (K^1_{ylL}= K^1_{ylR})	kN/m	1210
Lower vertical spring stiffness (K^2_{vlL}= K^2_{vlR}= K^3_{vlL}= K^3_{vlR})	kN/m	4400
Lower lateral spring stiffness (K^2_{ylL}= K^2_{ylR}= K^3_{ylL}= K^3_{ylR})	kN/m	2420
Lower vertical damper damping coefficient (C^1_{vlL}= C^1_{vlR})	kN·s/m	6.0
Lower lateral damper damping coefficient (C^1_{ylL}= C^1_{ylR})	kN·s/m	6.0
Lower vertical damper damping coefficient (C^2_{vlL}= C^2_{vlR}= C^3_{vlL}= C^3_{vlR})	kN·s/m	12.0
Lower lateral damper damping coefficient(C^2_{ylL}= C^2_{ylR}= C^3_{ylL}= C^3_{ylR})	kN·s/m	12.0
Reference area	m^2	10.5
Reference height	m	1.5
Distance (L_1)	m	3.1
Distance (L_2)	m	0.4
Distance (L_3)	m	1.8
Distance (b_1)	m	0.9
Distance (b_2)	m	0.0
Distance (h_1)	m	0.8
Distance (h_2)	m	1.0

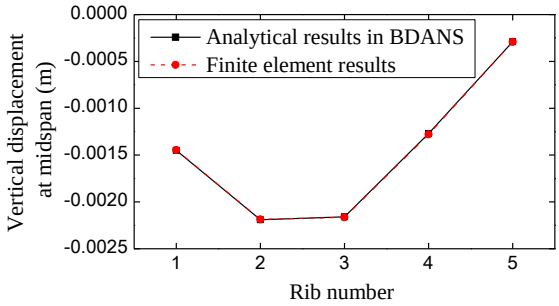

Fig. 8 Comparison of vertical displacements at mid-span between BDANS and ANSYS

4.2 Vehicle parameter

The truck model is illustrated in Fig. 6, and the properties, including the geometry, mass distribution, damping, and stiffness of the tires and suspension systems, are shown in Table 3. A modal analysis was conducted for the vehicle model. The first two frequencies of the vehicle are 2.658 Hz and 4.891 Hz, respectively, and both modes appear to be in the vertical direction.

5. Verification of the multi-girder vehicle-bridge coupling system analysis module

To verify the validity of the multi-girder vehicle-bridge coupling vibration analysis module in BDANS, the model of the rigid framed arch bridge was subjected to static loading and the simulated bridge response obtained in BDANS was compared to that of the bridge subjected to the same loading in the ANSYS program. The loading condition, including the longitudinal and transversal positions of the vehicle on the bridge, is illustrated in Fig. 7.

Fig. 8 shows the comparison of the vertical displacement at the mid-span for each rib between the results from BDANS and ANSYS. From the good agreements achieved between the results obtained from the two different programs in Fig. 8, it can be concluded that BDANS can achieve very good accuracy and can be used in the parametric study to predict the bridge dynamic response induced by moving vehicles.

6. The influence of input models on the vibration of the vehicle-bridge coupling system

6.1 The interaction force between the bridge and vehicle

The road roughness has a direct effect on the interaction force between the bridge and the vehicle, thus affecting the vibration of the vehicle-bridge coupling system. In order to study the influence of road surface roughness on the interaction forces of the vehicle-bridge coupling system, the following three cases for inputs are carried out in the numerical simulation respectively: (1) using the measured road roughness profile of the left wheel for the input of both wheels in the numerical simulation; (2) using the measured road roughness profile of the right wheel for both wheels; and (3) using the measured road roughness profiles corresponding to the

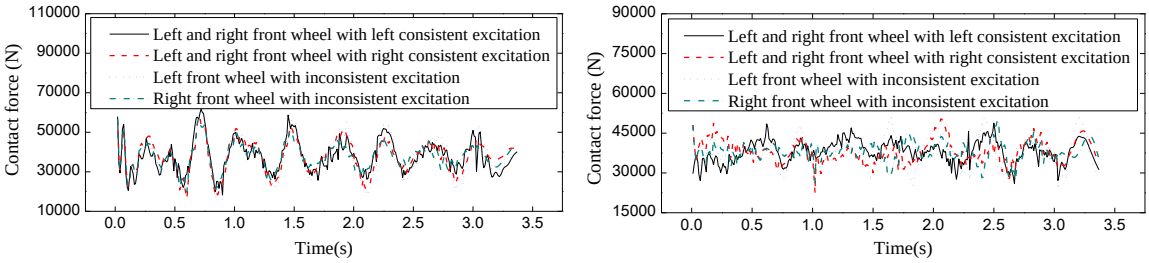

(a) Profile 1 (b) Profile 4

Fig. 9 Vertical contact force of front wheels using three input modes

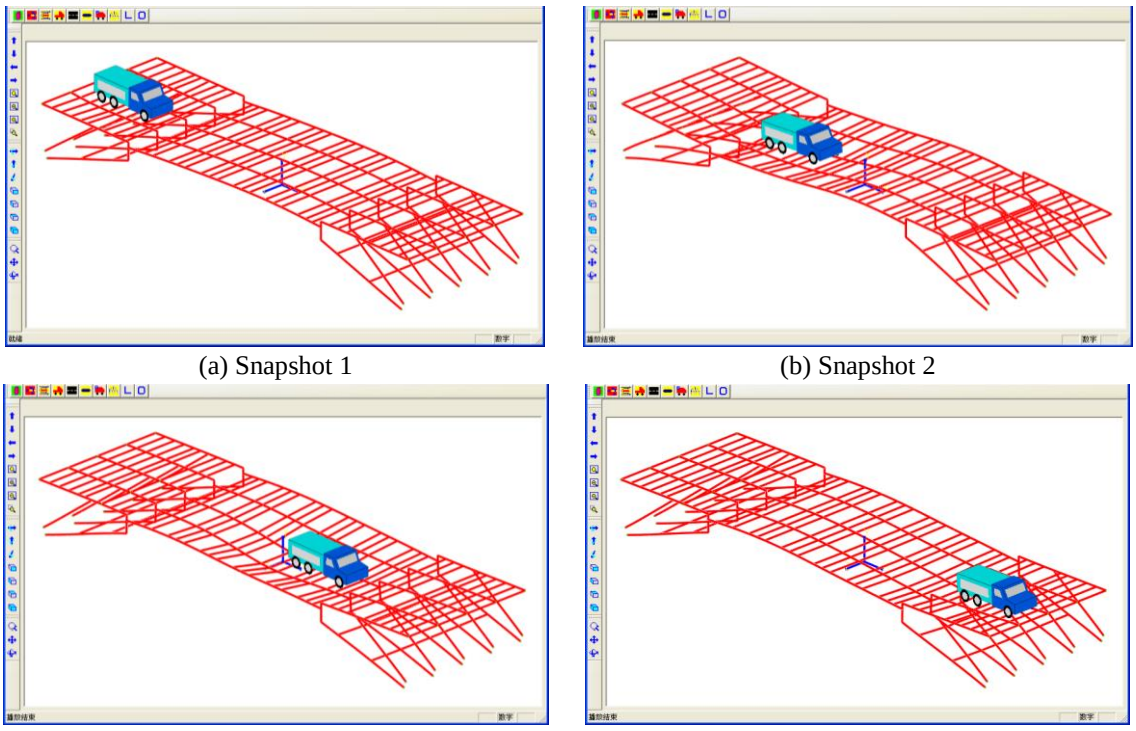

(a) Snapshot 1 (b) Snapshot 2

(c) Snapshot 3 (d) Snapshot 4

Fig. 10 Animation screenshot of the loading vehicle's driving through full bridge

left and right wheels for the input of the vehicle's left and right wheels, respectively. In the following sections, these three cases will be referred to as the left consistent excitation, right consistent excitation and inconsistent excitation, respectively.

Fig. 9 shows the interaction force time-history of vehicle's left and right front wheels at a speed of 50km/h under the three input modes with Profiles 1 and 4. It should be pointed out that since the road roughness profiles corresponding to vehicle's left and right wheels under consistent excitation are the same, the contact forces of vehicle's left and right wheels are identical for the cases of consistent excitation.

BDANS has a visualization display function that is able to display the responses of both the bridge and vehicle at any single time step during the process of a vehicle's driving across the

Table 4 Correlation coefficients between interaction force of left and right front wheels

Correlation coefficient	A and B	A and C	A and D	B and C	B and D	C and D
Profile 1	0.8201	0.9513	0.8449	0.8981	0.9259	0.8082
Profile 4	0.1019	0.6895	0.1379	0.5517	0.4183	-0.1950

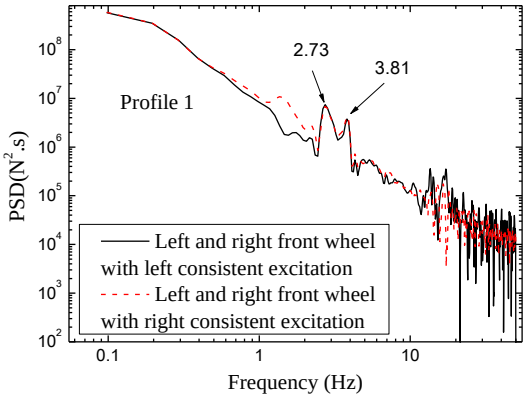

(a) Left and right consistent excitation with Profile 1

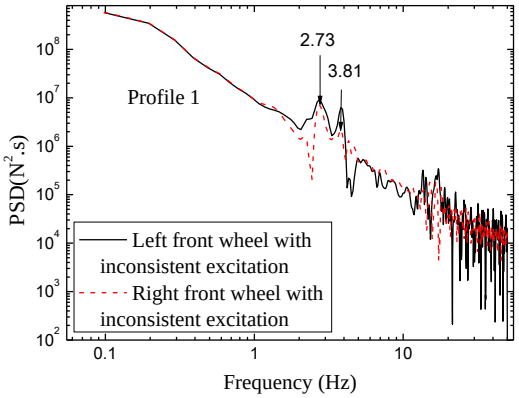

(b) Inconsistent excitation with Profile 1

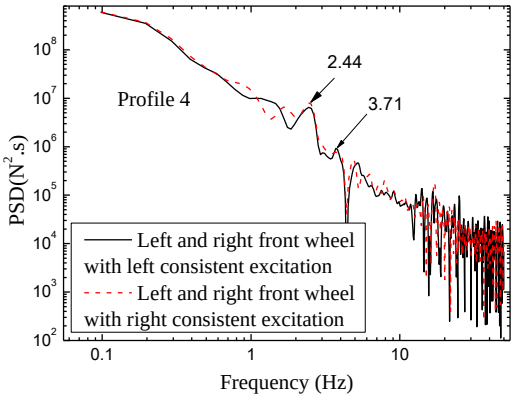

(c) Left and right consistent excitation with Profile 4

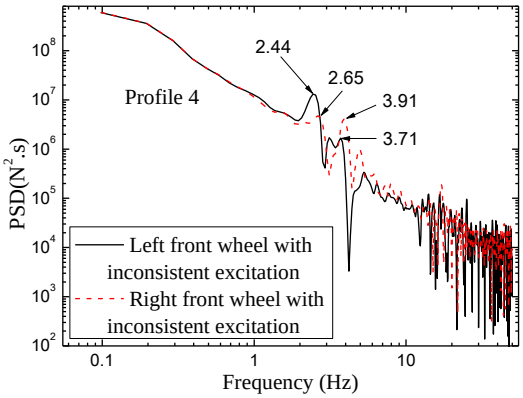

(d) Inconsistent excitation with Profile 4

Fig. 11 PSD of vertical contact forces of front wheel

bridge. The program can also animate this whole process on the screen. Fig. 10 shows the four snapshots during the process of the loading vehicle driving across the bridge at a speed of 50 km/h.

Table 4 shows the correlation coefficients between the interaction forces of the left and right front wheels with left consistent excitation (A), left and right front wheels with right consistent excitation (B), left front wheel with inconsistent excitation (C), right front wheel with inconsistent excitation (D) for the two sets of road roughness profiles selected

As shown in Fig. 9, the time histories of the four vertical contact forces for Profile 1 follow the same trend consistently while it is not the case for Profile 4. It can be seen from Table 4 that, for Profile 1, the largest correlation coefficient reaches 0.95 while the smallest correlation coefficient reaches 0.80 under the case of inconsistent excitation. For profile 4, however, the correlation between the four contact force time histories is much weaker, especially for the correlation between left and right wheels under inconsistent excitation, which is as low as -0.1950.

Table 5 Analysis of contact force of wheels with inputs of Profile 1 and Profile 4

		Left and right front wheel with left consistent excitation	Left and right front wheel with right consistent excitation	Left front wheel with inconsistent excitation	Right front wheel with inconsistent excitation
Profile 1	Mean value	37694.67	37797.41	37673.48	37819.02
	Variance	8203.98	8222.32	9902.09	6542.56
Profile 4	Mean value	38014.23	38043.60	37987.02	38071.79
	Variance	4161.87	4359.76	5969.70	3561.45

Fig. 11 shows the corresponding power spectral density of the vertical contact forces of the vehicle's left and right front wheels at a vehicle speed of 50 km/h under the three input cases corresponding for both Profiles 1 and 4.

It is observed from Fig. 11 that the two frequencies (2.73 Hz and 3.81 Hz) corresponding to the first two peak values of the PSD for contact forces of vehicle's left and right front wheels under the three input cases for the Profile 1 are the same. This may be attributed to the strong correlation between the road roughness profiles corresponding to the left and right wheels. Therefore, the spectral characteristic of vertical contact forces of wheels is generally consistent. In addition, these two frequencies are close to vehicle's vertical vibration fundamental frequency (2.66 Hz) and the bridge's vertical vibration fundamental frequency (4.26 Hz), respectively.

When the left and right consistent excitations were adopted using Profile 4, the frequencies corresponding to the first two peak values of the PSD for contact forces of vehicle's left and right front wheels are 2.44 Hz and 3.71 Hz, respectively. While the frequencies corresponding to two peak values of the PSD for contact force of vehicle's left front wheel under inconsistent excitation are 2.44 Hz and 3.71 Hz and those of right front wheel are 2.65 Hz and 3.91 Hz. There are some differences in spectral characteristics of vertical contact forces between left and right wheels. This may be attributed to the weak correlation between road surface roughness corresponding to left and right wheels for Profile 4.

Table 5 shows the statistic characteristics for interaction force under three input cases corresponding to Profile 1 and Profile 4. It can be seen from Table 5 that there is no apparent difference between Profile 1 and Profile 4 in terms of the mean value of contact force. The reason for this is probably that the mean value of interaction force is dependent on vehicle's weight distributed to the wheels. However, the variance of contact force of Profile 1 is twice as large as that of Profile 4.

6.2 Dynamic responses

When analyzing the vehicle-bridge coupling vibration for multi-girder bridges, the girder or rib that has the largest response should be selected for the analysis of impact factor. In this study, rib 2, which has the maximum response, was selected. Figs. 12-13 show the variation of vertical displacement DAF, vertical bending moment DAF, vertical acceleration RMS value at the bridge mid-span and vehicle body vertical acceleration RMS value with respect to vehicle speed under the three input modes for both Profiles 1 and 4.

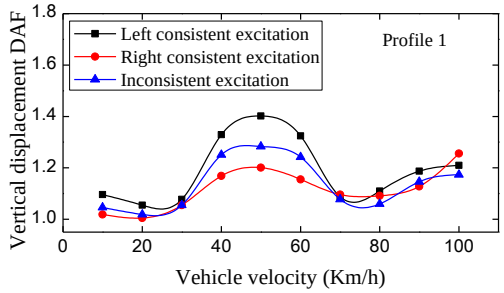

(a) Vertical displacement DAF

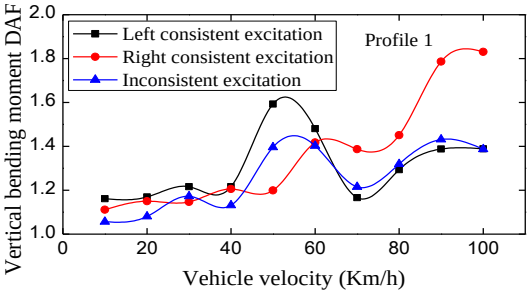

(b) Vertical bending moment DAF

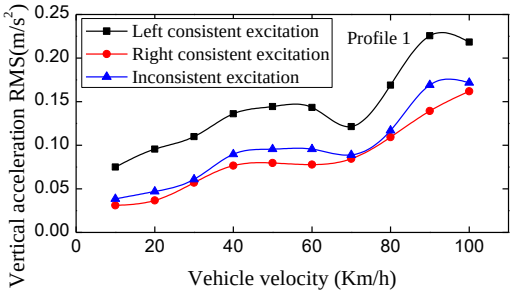

(c) Vertical acceleration RMS value

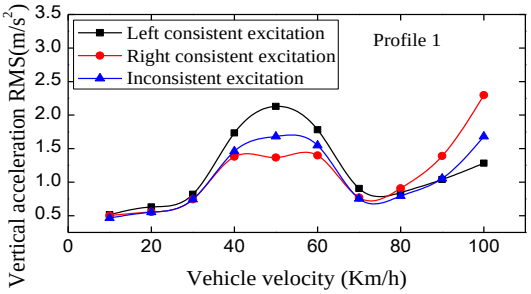

(d) Vehicle body vertical acceleration RMS value

Fig. 12 Dynamic responses of vehicle-bridge coupling system with Profile 1

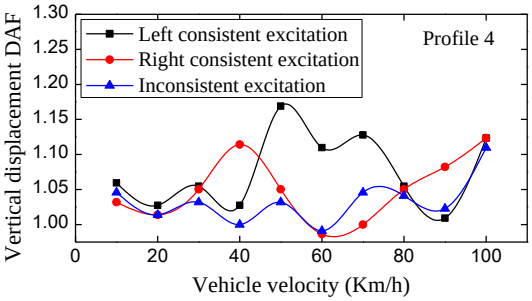

(a) Vertical displacement DAF

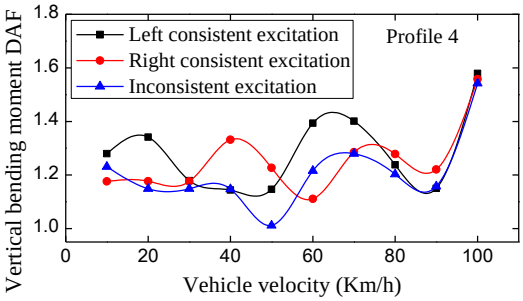

(b) Vertical bending moment DAF

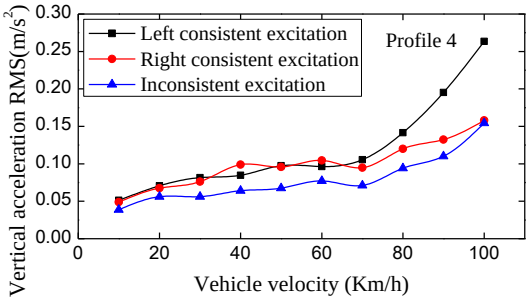

(c) Vertical acceleration RMS value

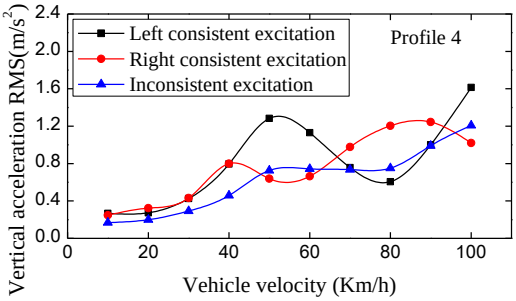

(d) Vehicle body vertical acceleration RMS value

Fig. 13 Dynamic responses of vehicle-bridge coupling system with Profile 4

It can be seen from Figs. 12-13 that, for Profile 1, the responses of the vehicle-bridge coupling system calculated using inconsistent excitation generally fall between the responses calculated

using the left and right consistent excitations; for Profile 4, the vehicle-bridge coupling system responses calculated using inconsistent excitation are smaller than those calculated using the left and right consistent excitations. In addition, the impact factor of rib 2 calculated using Profile 1 as input is apparently larger than that obtained using Profile 4. This is probably due to the fact that the variance of wheel contact force, i.e., the dynamic load amplitude, corresponding to Profile 1 is about twice as large as that corresponding to Profile 4.

6.3 Spectral characteristic

In order to study the influence of correlation between road roughness profiles of left and right wheels and excitation modes on spectral characteristic of vehicle-bridge coupling system, the time history of the vertical acceleration at the bridge mid-span and the vertical acceleration of the vehicle body as well as their corresponding PSD functions，at a vehicle speed of 50km/h, under the three input modes are shown in Figs. 14-15 for Profile 1 and 4, respectively.

It can be observed from Fig. 14(b) that, when Profile 1 is used, the first peak frequencies on the PSD curves for the vertical acceleration at bridge mid-span are 2.73 Hz, 2.83 Hz and 2.73 Hz, corresponding to the three different input modes, respectively. It is noted that these three frequencies are very close to the fundamental vibration frequency of the vehicle (in the vertical direction, =2.66 Hz). It can also be observed that the second peak frequencies on the three PSD curves are 4.00 Hz, 4.29 Hz and 4.00 Hz, all of which are close to the bridge's fundamental frequency of 4.26 Hz.

From Fig. 14(d), it can be observed that the peak frequencies on the three PSD curves for the vertical acceleration of the vehicle body are 2.54 Hz, 2.50 Hz and 2.64 Hz, corresponding to the three different input modes, respectively. These peak frequencies are very close to the fundamental

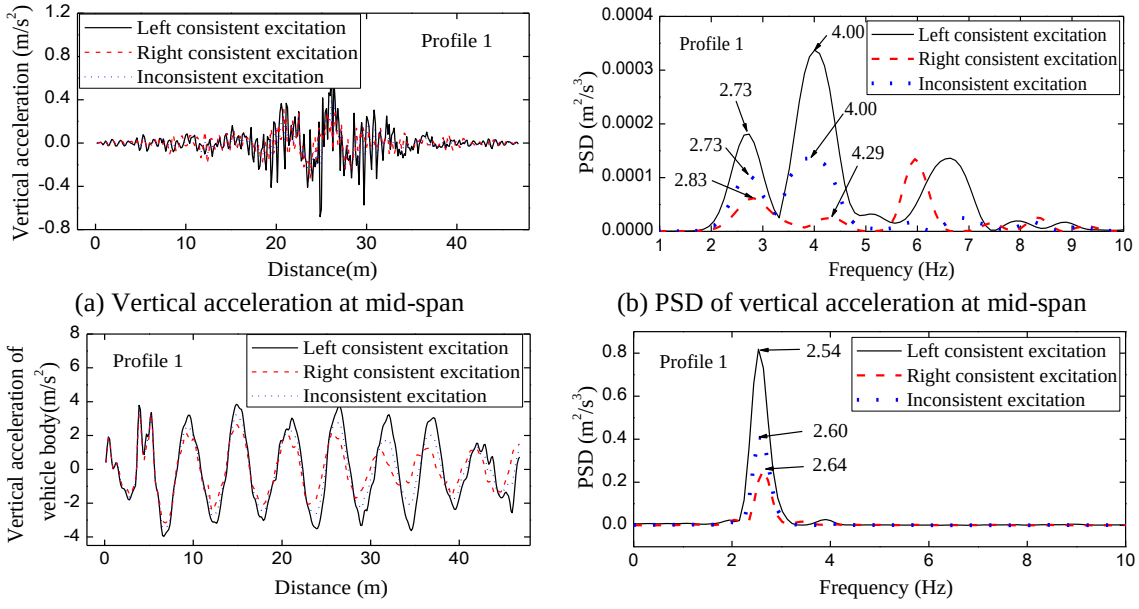

(a) Vertical acceleration at mid-span

(b) PSD of vertical acceleration at mid-span

(c) Vertical acceleration of vehicle body

(d) PSD of vertical acceleration of vehicle body

Fig. 14 Acceleration responses and PSD analysis with Profile 1

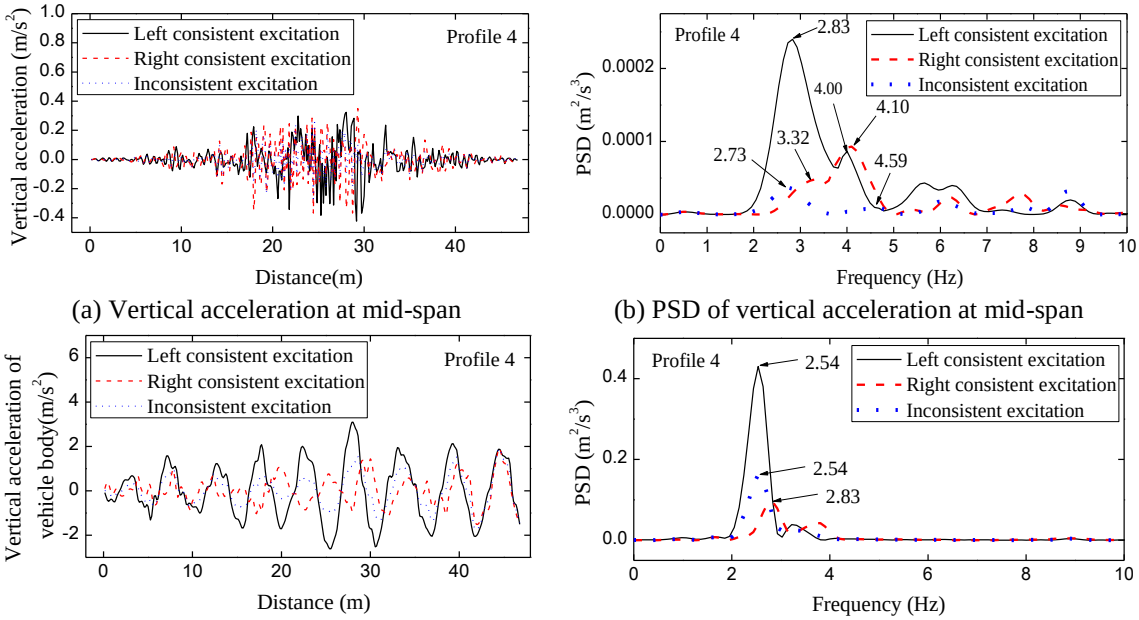

(a) Vertical acceleration at mid-span

(b) PSD of vertical acceleration at mid-span

(c) Vertical acceleration of vehicle body

(d) PSD of vertical acceleration of vehicle body

Fig. 15 Acceleration responses and PSD analysis with Profile 4

frequency of the vehicle (2.66 Hz).

Similar results can be observed from the results when Profile 4 is used as input, as can be seen from Fig. 15(b) and 15(d). However, it is also noted that though the three first-peak frequencies (2.83 Hz, 3.32 Hz and 2.73 Hz) in Fig. 15(b) are close to the natural frequency of the vehicle, the discrepancies between these three frequencies have become larger than the discrepancies when Profile 1 is used. This trend can also been confirmed on the second peak frequencies for the vertical acceleration of the bridge mid-span (Fig. 15(b)) and the peak frequencies for the vertical acceleration of the vehicle body (Fig. 15(d)). This phenomenon may be explained by the fact that the correlation of the two road roughness profiles corresponding to the left and right wheels in Profile 1 is stronger than the correlation in Profile 4.

7. Conclusions

This study has investigated the correlation of measured road roughness profiles corresponding to the left and right wheels of a vehicle. The influence of different road roughness input modes on the vibration of the vehicle-bridge coupling system was investigated. Based on the results from the numerical simulations using two sets of road roughness profile selected and the three different input modes, the following concluding remarks can be made:

1) There is significant discrepancy in the correlation of the two road roughness profiles corresponding to the left and right wheels of a vehicle based on the four sets of roughness profiles measured, with the coefficient of correlation ranging from 0.0988 to 0.8778. It is very interesting to find that all the four coefficients of correlation are positive. Furthermore, difference has been found between the power spectral density (PSD) functions of the road roughness profiles

corresponding to the left and right wheels.

2) When the correlation between road roughness corresponding to left and right wheels is strong, the magnitudes of the responses of the vehicle-bridge coupling system calculated by using the inconsistent excitation are within the ranges that can be predicted by using the two consistent input modes.

3) The road roughness correlation coefficient affects the dynamic characteristics of the bridge response under different road roughness input modes. The peak frequencies on the PSD curves tend to have smaller variations when the road roughness correlation coefficient becomes stronger. The discrepancies between the peak frequencies on the PSD curves of the vehicle-bridge system and the natural frequencies of the vehicle and bridge become larger when the road roughness correlation coefficient becomes smaller.

Acknowledgments

The authors acknowledge the financial contribution by Grant of national natural science foundation (51278064) and Fundamental Research Funds for the Central Universities (2013G2211002).

References

Au, F.T.K., Cheng, Y.S. and Cheung, Y.K. (2001), "Effects of random road surface roughness and long-term deflection of prestressed concrete girder and cable-stayed bridges on impact due to moving vehicles", *Comput. Struct.*, **79**(8), 853-872.

Calcada, R., Cunha, A. and Delgado, R. (2005), "Analysis of traffic-induced vibrations in a Cable-stayed bridge Part I: Experimental Assessment", *J. Bridge Eng.*, **10**(4), 370-385.

Cai, C.S., Shi, X.M., Araujo, M. and Chen, S.R. (2007), "Effect of approach span condition on vehicle-induced dynamic response of slab-on-girder road bridges", *Eng. Struct.*, **29**(12), 3210- 3226.

Dodds, C.J. and Robson, J.D. (1973), "The description of road surface roughness", *J. Sound Vib.*, **31**(2), 175-183.

Ding, L.N., Hao, H. and Zhu, X.Q. (2009), "Evaluation of dynamic vehicle axle loads on bridges with different surface conditions", *J. Sound. Vib.*, **323**(3-5), 826-848.

Guo, W.H. and Xu, Y.L. (2001), "Fully computerized approach to study cable-stayed bridge-vehicle interaction", *J. Sound. Vib.*, **248**(4), 745–761.

Huang, D.Z., Wang, T.L. and Shahawy, M. (1992), "Impact studies of multigirder concrete bridges", *J. Struct. Eng.*, **118**(12), 3427-3443.

Han, W.S. (2006), "Three-dimensional coupled vibration of wind-vehicle-bridge system", Ph.D. Dissertation, Tongji Universiy, Shanghai.

International Organization for Standardization (ISO) (1995), "Mechanical Vibration-Road Surface Profiles-Reporting of measured Data", ISO 8068: (E), ISO, Geneva.

Kim, C.W., Kawatani, M. and Kwon, Y.R. (2007), "Impact coefficient of reinforced concrete slab on a steel girder bridge", *Eng. Struct.*, **29**(4), 576-590.

Liu, C.H., Huang, D.Z. and Wang, T.L. (2002), "Analytical dynamic impact study based on correlated road roughness", *Comput. Struct.*, **80**(20-21), 1639-1650.

Ministry of Communication of China (1982), *Load Test Methods of Long Span Concrete Bridge*, China Communications Press, Beijing, China.

Obrien, E., Li, Y.Y. and Gonza'lez, A. (2006), "Bridge roughness index as an indicator of bridge dynamic

amplification", *Comput. Struct.*, **84**(12), 759-769.
Wang, T.L. and Huang, D.Z. (1992), "Cable-stayed bridge vibration due to road surface roughness", *J. Struct. Eng.*, **118**(5), 1354-1374.
Wang, T.L., Liu, C.H., Huang, D.Z. and Shahawy, M. (2005), "Truck loading and fatigue damage analysis for girder bridges based on weigh-in-motion data", *J. Bridge Eng.*, **10**(1), 12-20.
Xu, Y.L. and Guo, W.H. (2004), "Effects of bridge motion and crosswind on ride comfort of road vehicles", *J. Wind Eng. Indus. Aerodyn.*, **92**(7-8), 641- 662.
Yang, Y.B., Li, Y.C. and Chang, K.C. (2013), "Effect of road surface roughness on the response of a moving vehicle for identification of bridge frequencies", *Interact. Multisc. Mech.*, **46**(1), 347- 368.
Zhu, J.S., Chen, C. and Han, Q.H. (2014), "Vehicle-bridge coupling vibration analysis based fatigue reliability prediction of prestressed concrete highway bridges", *Struct. Eng. Mech.*, **49**(2), 203- 223.